

Profit maximization of the normal hexane recovery process through a thermal integration method

Hye-Ran Kim*, Dong Sun Kim**,†, and Jungho Cho**

*Department of Business Management, Hongik University, 300, Shinan-ri, Jochiwon-up, Yongi-gun, Chungnam 339-701, Korea

**Department of Chemical Engineering, Kongju National University, 275, Budae-dong, Cheonan, Chungnam 330-717, Korea

(Received 30 September 2011 • accepted 25 December 2011)

Abstract—We developed a separation process that can minimize utility consumption in order to obtain normal hexane from crude raffinates for electronic-grade reagents. For the separation of normal hexane from the crude raffinate mixtures, a two-column configuration was selected. The first distillation column removes lighter constituents than normal hexane as a column top product, after which heavier constituents containing normal hexane are put into the middle of the second distillation column. This allows normal hexane with a purity of 95.5 wt% to be obtained from the top of the second distillation column by removing the constituents that are heavier than normal hexane as a second column bottom product. When both distillation columns are operated at approximately atmospheric pressure, it requires about 5.2 tons of steam per hour both for the reboiling heating source. However, when the operating pressure of the second distillation column is increased, the vapor stream coming out of the top of the second distillation column can be used as a heating medium for the reboiling source of the first distillation column. In this way, steam of only 3.1 tons per hour is required, potentially reducing the amount of steam used to 59.6% of the original amount.

Key words: Normal Hexane Recovery, Energy Saving, Simulation NRTL Liquid Activity Coefficient Model, Optimization

INTRODUCTION

As normal hexane is an electronic reagent, it is used as a cleaning solvent in semiconductor processes. In this study, we conducted process simulations to recover 92% of normal hexane from the crude raffinates, which contains approximately 64.0 wt% of normal hexane. Purified normal hexane purity should be more than 95.5 wt% and at a rate of more than 625 kg/h. Table 1 shows the feed compositions of the raw material and the properties of the crude raffinates.

To separate normal hexane from the mixture of raw materials, the 2MP and 3MP components, which are lighter than normal hexane, and the MCP and benzene constituents, which have higher boiling points than normal hexane, should be removed. We could consider two different distillation processes that could separate normal hexane, which has a mid-range boiling point, by removing the 2MP and 3MP constituents, which have lower boiling points, and by remov-

ing the MCP and benzene constituents, which have higher boiling points. In the first distillation process, the 2MP and 3MP constituents are produced as a top product steam in a first distillation column, sending normal hexane and heavier constituents with higher boiling points than normal hexane to a second distillation column to obtain normal hexane-rich stream as a top product in a second distillation column, by removing the heavier constituents at the bottom of the second distillation column. As shown in Fig. 1, this process is known as the direct sequence process [1]. The raw material of the crude raffinates is taken from the TK-101 tank to the middle of the C-101 distillation column by P-101A/B pumps. The 2MP and 3MP constituents, which are lighter than normal hexane, are removed at the top of the C-101 column. The normal hexane stream, with a 95.5 wt% purity rating, can be obtained as the top product of the C-102 column, the second distillation column. The MCP and benzene constituents with higher boiling points than normal hexane are removed as the bottom product of the second distillation column. On the other hand, in Fig. 2, MCP and constituents heavier than normal hexane are removed at the bottom of C-101, the first distillation column, and 2MP and 3MP including normal hexane are obtained at the top and sent to the middle of the second distillation column, where constituents with a boiling point lower than that of normal hexane are removed from the top distillate, and where normal hexane is extracted as a bottom product of the second distillation column. This process is known as the indirect sequence process [2]. It is generally known that the process arrangement of the direct sequence can reduce the energy consumption of the process than that of the indirect sequence.

The primary objective of this study is to maximize the profit potential of the normal hexane recovery process through a thermal integration method. For the modeling of the normal hexane recov-

Table 1. Feedstock properties

Crude raffinate feed		NBP (°C)
Component (abbreviation)	Weight%	
2-Methyl pentane (2MP)	0.41	60.26
3-Methyl pentane (3MP)	6.10	63.27
Normal hexane (NC6)	64.00	68.73
Methyl cyclopentane (MCP)	25.80	71.81
Benzene (benzene)	3.69	80.09

†To whom correspondence should be addressed.

E-mail: dskim@kongju.ac.kr

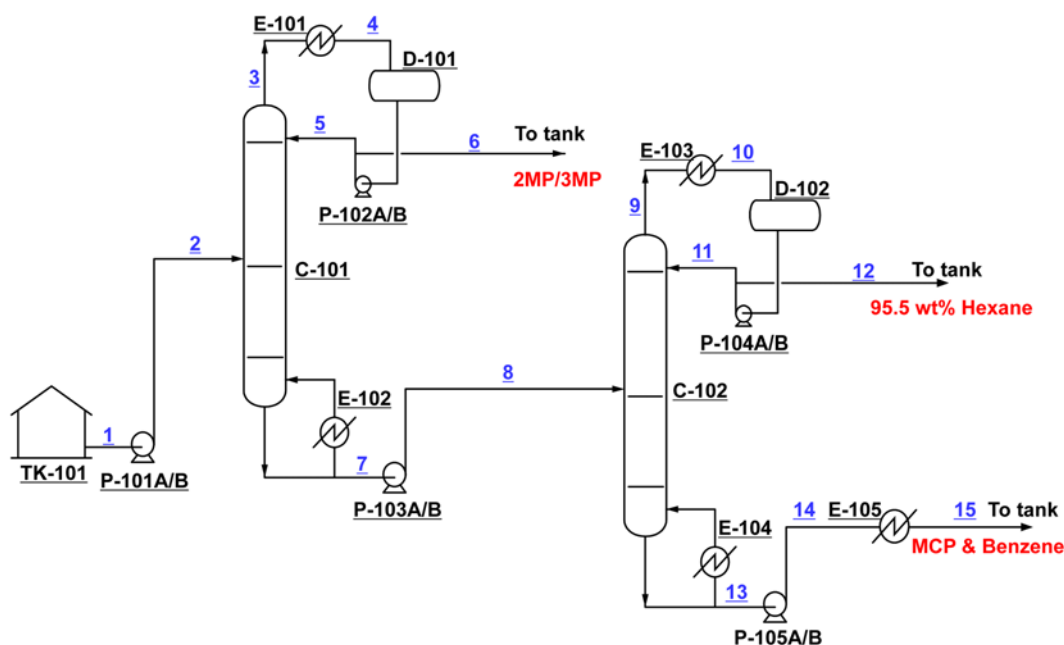


Fig. 1. Direct sequence for the recovery of normal hexane.

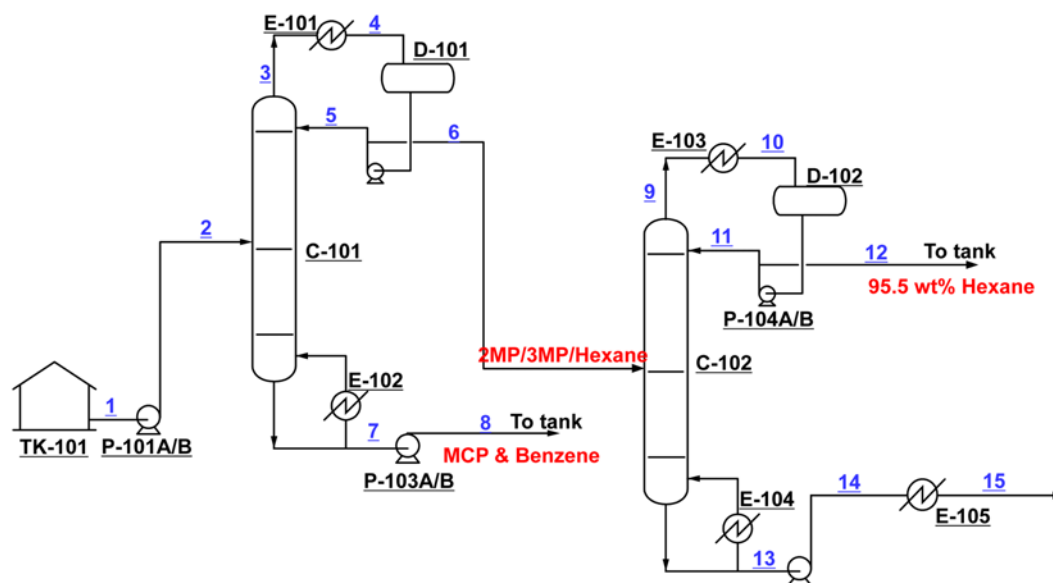


Fig. 2. Indirect sequence for the recovery of normal hexane.

ery process, PRO/II with PROVISION 9.0 [3] was used. In addition, the NRTL liquid activity coefficient model proposed by Renon and Prausnitz [4] was selected as a suitable thermodynamic model.

THERMODYNAMIC THEORY

The starting point in a calculation of the vapor-liquid equilibria in mixtures requires the fugacities to be identical in each phases for any component ‘i’ in a mixture. This can be expressed as Eq. (1):

$$\hat{f}_i^v(T, P, y_i) = \hat{f}_i^l(T, P, x_i) \quad (1)$$

There are two approaches that can be used to calculate the vapor-

liquid equilibria. The first approach is to use an equation of state model for the estimation of the vapor- and liquid-phase fugacity coefficients. This approach is known as a one-model approach, as the same tool, the equation of state model, is used both for the calculation of the vapor and liquid phases. The second approach is to use liquid activity coefficient models for the calculation of the liquid phase activity coefficients. In this case, the vapor phase should be assumed to be ideal. Otherwise the equation of state model can be used to estimate the vapor phase non-idealities. Such an approach is termed a two-model approach. In this work, we used the two-model approach. The starting equations for the two-model approach are as follows:

$$\hat{f}_i^v(T, P, y_i) = \hat{\phi}_i^v y_i P \quad \text{for the vapor phase} \quad (2a)$$

$$\hat{f}_i^l(T, P, x_i) = \gamma_i x_i P_i^{vap} \quad \text{for the liquid phase} \quad (2b)$$

A typical example of the two-model approach is to use an equation of state model, such as the Soave-Redlich-Kwong [5] or Peng-Robinson model [6] to estimate the vapor-phase fugacity coefficient and a liquid activity coefficient model such as the Wilson [7], UNIQUAC [8] or UNIFAC model [9]. If the operating pressure of the distillation column is lower than 10 bars, we can assume that the vapor phase behaves ideally as long as there are no associating constituents such as acetic acid or hydrogen fluoride. The activity coefficient in the liquid phase from Eq. (2b) can be expressed as Eq. (3):

$$\ln \gamma_i = \left[\frac{\partial (nG^{ex}/RT)}{\partial n_i} \right]_{T, P, n_j} \quad (3)$$

To estimate the liquid phase activity coefficient, we used the NRTL model. The NRTL liquid activity coefficient model is expressed as Eq. (4):

$$\ln \gamma_i = \frac{\sum_j \tau_{ji} G_{ji} x_j}{\sum_k G_{ki} x_k} + \sum_j \frac{x_j G_{ij}}{G_{ij} x_k} \left(\tau_{ij} - \frac{\sum_k x_k \tau_{kj} G_{kj}}{\sum_k G_{kj} x_k} \right) \quad (4)$$

where,

$$\tau_{ij} = a_{ij} + \frac{b_{ij}}{T} \quad (5)$$

$$G_{ij} = \exp(-\alpha_{ij} \tau_{ij}) \quad (6)$$

Table 2 shows the NRTL binary interaction parameters for two major binary pairs, 3MP+NC6 and NC6+MCP. For each binary

Table 2. NRTL binary interaction parameters

Component i	Component j	a_{ij}	a_{ji}	α_{ij}
3MP	NC6	136.7270	-101.0150	0.3040
NC6	MCP	65.6881	-51.1244	0.3037

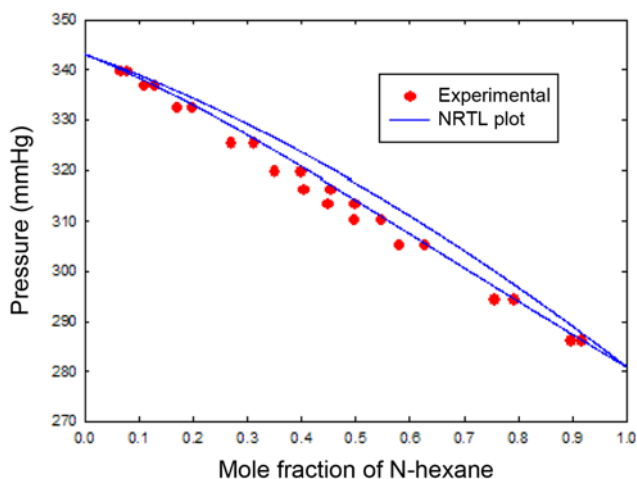


Fig. 3. Isothermal binary experimental data for normal hexane and 3-methyl pentane at 313.15K and its prediction with the NRTL model.

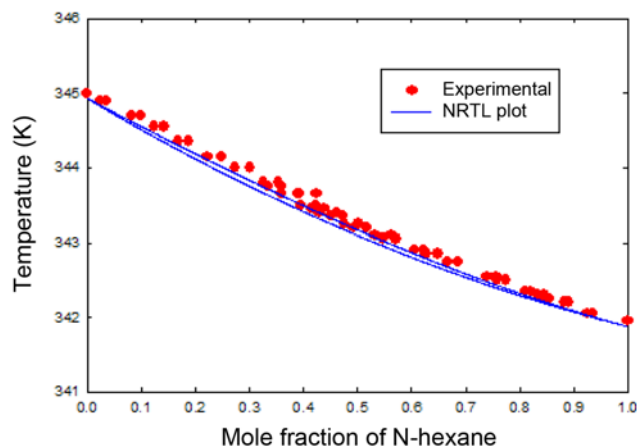


Fig. 4. Isobaric binary experimental data for normal hexane and methyl cyclopentane at 1.013 bar and its prediction with the NRTL model.

pair, the NRTL liquid activity coefficient model has three binary interaction parameters, a_{ij} , a_{ji} and α_{ij} .

Fig. 3 shows a plot of the isothermal binary experimental data of the vapor-liquid equilibria expressing the pressure vs. composition for normal hexane and 3-methyl pentane at 313.15 K [10] and its predictions with the NRTL model. Fig. 4 shows the binary isobaric experimental vapor-liquid equilibria data for normal hexane and methyl cyclopentane at 1.013 bar [11] and its prediction with the NRTL model. For binary interactions other than the major binary interactions, we estimated the activity coefficients with the UNIFAC model equation.

PROCESS SIMULATIONS

1. The Arrangements of Distillation Processes Using the Thermal Integration Method

Fig. 5 shows an improved version of the direct sequence shown in Fig. 1, as the hot vapor stream coming out of the top of the second distillation column can be used as a heating source to reboil the first distillation column. As the pressure for the second distillation column is increased from atmospheric pressure to 2.59 bars, the vapor temperature of the top stream increases to 102.4 °C. The top vapor stream from the second distillation column is then higher by about 20 °C than 82.4 °C, the bottom temperature of the first distillation column. Therefore, we can conserve the hot utility, steam for the reboiler heat source of the first distillation column, along with the cold utility, the cooling water for the condenser cooling medium of the second distillation column, though a thermal integration process.

2. Calculations of the Minimum Number of Theoretical Stages and Minimum Reflux Ratio, and Determination of the Optimum Number of Theoretical Stages

To determine the minimum number of theoretical stages and minimum reflux ratio for each distillation column to separate the normal hexane from the raffinate crude, we used the shortcut module built-in PRO/II with PROVISION release 9.0. Table 3 shows the specifications used for each column for the shortcut calculations.

The minimum number of theoretical stages for the C-101 col-

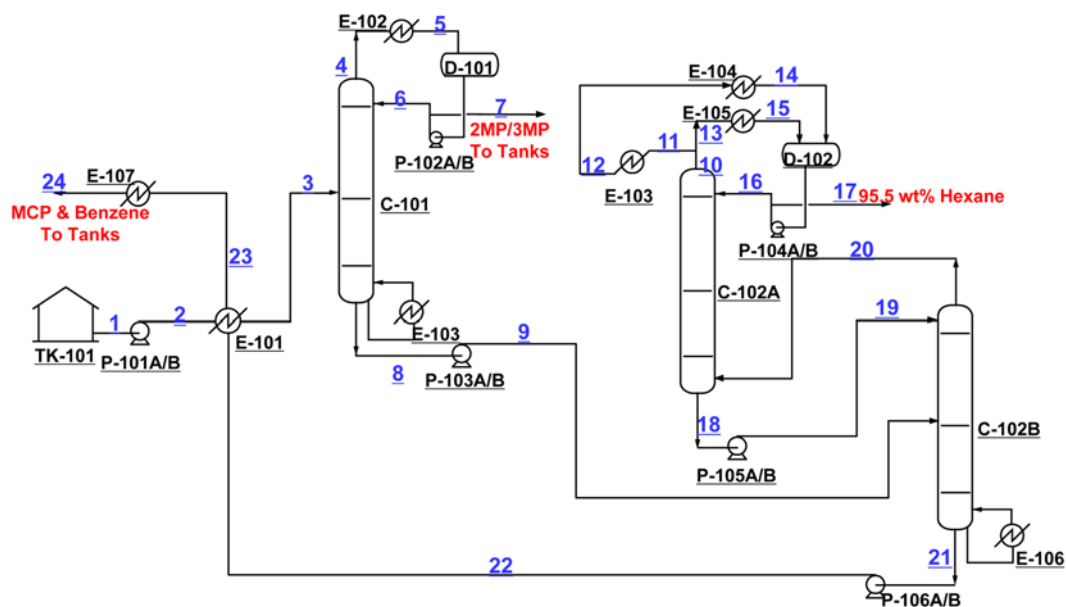


Fig. 5. Overview of the normal hexane separation process utilizing the heat integrated distillation processes.

Table 3. Product specifications for each distillation column

Column	Stream	Specifications
C-101	Top	Mass flow rate=66 kg/h Weight% for 2MP+3MP=95
C-102	Top	Recovery ratio for original feed=0.92 Normal hexane weight%=95.5

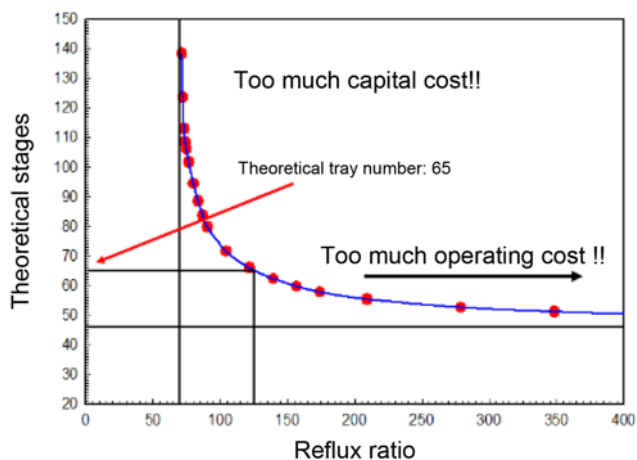


Fig. 6. Plot of the theoretical number of stages versus the reflux ratio for column C-101.

umn was 46 and the minimum reflux ratio was about 70. Fig. 6 shows the relationship between the theoretical number of stages and the reflux ratio for the C-101 column. The reflux ratio and theoretical stage relationships in Fig. 6 show that the theoretical number of stages is inversely proportional to the reflux ratio. When a distillation column is operated at higher reflux ratio, it requires fewer trays, possibly lowering the initial capital cost of the process, while increasing the operating cost. On the other hand, a distillation column with

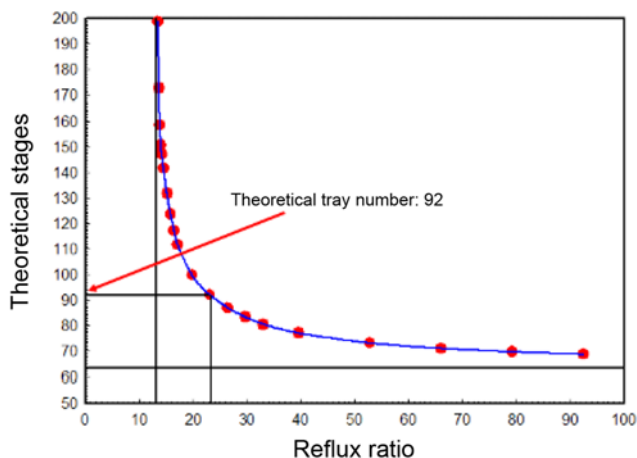


Fig. 7. Plot of the theoretical number of stages versus the reflux ratio for column C-102.

a lower reflux ratio may cost less to operate, but because the number of theoretical stages increases, the initial capital cost for the process will also increase. Fig. 6 shows that the total investment cost (the sum of the operation cost and the initial capital cost of the process) is minimal where the theoretical stages vs. the reflux ratio curve sharply declines. The optimal reflux ratio is about 125 and the optimum number of theoretical stages is about 65 including the top condenser and bottom reboiler.

Fig. 7 depicts the relationship between the theoretical number of stages vs. the reflux ratio for the C-102 column. According to Fig. 7, the optimal reflux ratio is approximately 23 and the optimum number of theoretical stages is about 92.

Table 4 shows the mass balance results for the shortcut modeling. According to the mass balance in Table 4, that the purity of normal hexane is 95.5 wt% at the top stream of the second distillation column, the recovery ratio for the raw material is 92%, and the pro-

Table 4. Mass balance for the shortcut modeling

Stream name	Feed		Top of the first column		Top of the second column		Bottom of the second column	
Component	kg/h	wt%	kg/h	wt%	kg/h	wt%	kg/h	wt%
2MP	4.1562	0.4100	5.1145E-4	0.0000	5.1145E-4	0.0000	0.0000	0.0000
3MP	61.8366	6.1000	3.2924	0.3474	3.2924	0.5268	0.0000	00000
NC6	648.7773	64.0000	645.5181	68.1131	596.8752	95.5000	48.6430	15.0731
MCP	261.5383	25.8000	261.5155	27.5943	23.4854	3.7577	238.0299	73.7587
Benzene	37.4061	3.6900	37.3881	3.9451	1.3466	0.2155	36.0415	11.1682
Flow rate (kg/h)	1,013.7145	100.0000	947.7145	100.0000	625.0002	100.0000	322.7144	100.0000

duction rate of normal hexane with the 95.5 wt% purity is 625 kg/h.

3. Rigorous Simulation

The optimum number theoretical stages was determined by the case study outlined in section 3.2 using the inverse relationship between the number of theoretical stages and the reflux ratio with the shortcut module. However, according to the process arrangement in Fig. 3, mixed raw materials are introduced into the middle of the C-101 column (the first distillation column) after being pre-heated by the E-101 heat exchanger. Constituents with a boiling point lower than normal hexane, in this case 2MP and 3MP, are removed at stream number 7, which is the top product stream of the first distillation column. Then normal hexane and heavier constituents are then fed into the C-102B column, at the lower part of this second distillation column. We divided the C-101 second distillation column into upper and lower parts because the second distillation column has too many stages. The bottom products from the first distillation column are pressurized by a P-103A/B pump, and are introduced into the middle of the C-102B column. The operating pressure for the top of the second distillation column is 2.59 bars, which is enough to increase the temperature of the top vapor stream of the second distillation column so that it can be used as the heating source of the first column reboiler. We can obtain normal hexane with a purity of 95.5 wt% at a production rate of 625 kg/h and a recovery ratio of 92% of recovery ratio from the raw material as a top product stream at the lower part of the second distillation column. In the bottom of

the lower column, constituents with a boiling point lower than that of normal hexane are removed and the stream is cooled to 45 °C by an E-107 heat exchanger, after which they are sent to a storage tank. Fig. 8 shows the estimated tray efficiency for each column as a function of the liquid feedstock average viscosity [12]. Because average viscosity of the raw material is about 0.19 cP, the estimated tray efficiency is 62%.

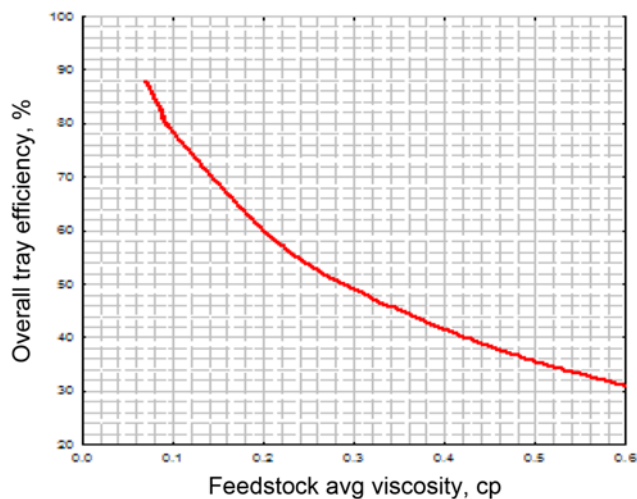


Fig. 8. Tray efficiency estimation for each column as a function of the average of the liquid feedstock.

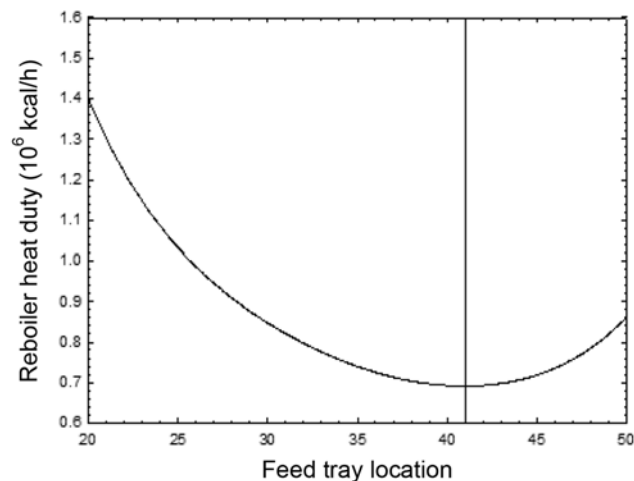


Fig. 9. Determination of the optimal feed tray location that minimizes the reboiler heat duty for the C-101 column.

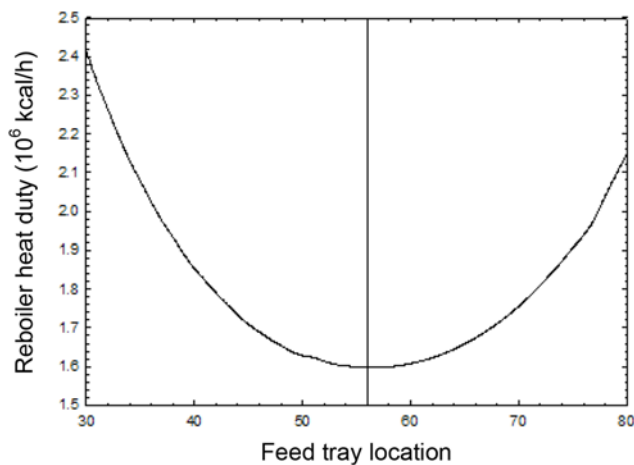


Fig. 10. Determination of the optimal feed tray location that optimally minimizes the reboiler heat duty for C-102 column.

Fig. 9 shows the relationship between the feed tray location and the reboiler heat duty for the C-101 first distillation column. This figure shows that the feed tray location that optimally minimizes the reboiler heat duty is 41. At the optimal feed tray location, the minimum reboiler heat duty is 0.69×10^6 kcal/h.

Fig. 10 also shows the relationship between the feed tray location and the reboiler heat duty for the C-102 second distillation column. This figure shows that the feed tray location that optimally minimizes the reboiler heat duty is 41. At the optimal feed tray, the minimum reboiler heat duty is 1.5970×10^6 kcal/h. Fig. 10 shows the change in heat duty of the reboiler as the feed stage to the second distillation column increases from tray number 30 to 80. The heat duty of the reboiler decreases as the position of the raw material input shifts from the top to bottom until it reaches 56 trays (minimal point) and increases again. Fig. 10 shows that when the feed stream is introduced at the tray number 56, the minimum reboiler heat duty is 1.5970×10^6 kcal/h.

Table 5 is a summary of the design conditions required when conducting the process simulation. As shown, we fixed the theoretical stage for the C-101 distillation column at 63 trays, excluding the condenser and reboiler. Because the tray efficiency was 62%, we fixed the actual number of stages at 102 trays. We also set the operating pressure of the first distillation column to atmospheric pressure. The type of condenser was the sub-cooled type, and the column

internal type was a valve tray. We assumed that the theoretical number of stages of the C-102 column, the second distillation column, was 90 trays excluding the condenser and reboiler. Considering that this made the tray efficiency 62%, we fixed the actual number of stages at 146 trays, and fixed the actual number of stages for upper column and lower column at 73 trays. However, we set the operating pressure of the top of the upper column at 2.59 bars. The cooling water supply temperature was 32 °C and the return temperature was 40 °C. Finally, we assumed that the steam was supplied under a saturated condition of 10.0 kg/cm²G for the reboiling heat source of the second distillation column.

In conclusion, by increasing the operating pressure of the second distillation column from atmospheric pressure to 2.59 bars and by integrating the hot vapor stream of the second distillation column top thermally with the reboiler of the first distillation column, the required hot utility, steam for the reboiler of the first distillation column and the cold utility, cooling water for the condenser of the second distillation column were conserved. Table 6 summarizes the consumption amount of the cooling water and the steam.

As shown in Table 6, because the heat exchanger in E-101 exists between the process streams, it can recover 1.099×10^{-2} kcal/h. In addition, 0.6900 kcal/h, the first column reboiler heat duty, can be saved through an exchange of heat with the top vapor stream of the second distillation column. This implies that we can reduce the

Table 5. Design conditions for each column

Column	C-101 column	C-102 column
Theoretical stage number	63	90
Reflux ratio	Manipulated	Manipulated
Tray efficiency	62%	62%
Actual stage number	102	146
Feed stage location from the top	42	56
Condenser type	Sub-cooled	Sub-cooled
Condenser temperature	45 °C	45 °C
Cooling water supply temperature	32 °C	32 °C
Cooling water return temperature	40 °C	40 °C
Steam condition	10.0 kg/cm ² G saturated	10.0 kg/cm ² G saturated
Condenser pressure	1.05 bar	2.59 bar
Column top pressure	0.2 bar	0.2 bar
Column pressure drop	0.3 bar	0.3 bar
Internal type	Valve tray	Valve tray

Table 6. Consumed amounts of cooling water and steam for each heat exchanger

Equipment ID	Equipment name	Heat duty (106 kcal/h)	Utility	Cooling water consumptions (ton/hr)	Steam consumptions (kg/hr)
E-101	Feed pre-heater	1.099E-02	Recovery		
E-102	1 st Column condenser	0.6730	c/w	84.17	
E-103	C-101 Reboiler	0.6900	Recovery		
E-104	2 nd Column condenser 1	0.2250	c/w	28.10	
E-105	2 nd Column condenser 2	0.6910	c/w	86.33	
E-106	2 nd Column reboiler	1.5970	Steam		3,335
E-107	Heavy product cooler	2.634E-04	c/w	(32.93 Kg/hr)	
Total				198.60	3,335

Table 7. Column simulation results summary

Column	C-101 column	C-102 column
Reflux ratio	106.6	22.8
Reflux molar rate (kmol/h)	85.3	166.7
Feed stage location from top	42	57
Condenser duty (10^6 kcal/h)	-0.6730	-1.6060
Cooling water consumption (ton/h)	84.17	114.43
Column top temperature ($^{\circ}$ C)	68.8	102.4
Reboiler duty (10^6 kcal/h)	0.6900	1.5970
Column bottom temperature ($^{\circ}$ C)	82.4	112.4
Reboiler return temperature ($^{\circ}$ C)	82.6	112.5
Steam consumption (kg/h)	Recovery	3,335
Flooding percent (%)	85	85
Tray spacing (mm)	610	610
Column efficiency (%)	62	62

steam consumption by about 1,346 kg/hr of 10.0 kg/cm²G saturated steam. Without the thermal integration process, a total of 4,681 kg/h would be consumed, meaning that we can reduce steam usage by about 28.8%. Moreover, with the use of the reboiler from the top of the distillation column as a source of heat, the cold utility must be used, with cooling water in order to cool, allowing a reduction of about 84 ton/h of cooling water. Without the thermal integration process, the system would consume a total of 284 tons/h of cooling water, indicating that approximately 30% of the cooling water can be conserved.

Table 7 shows the results of the process simulation and the optimization conditions for the normal hexane recovery process. The second distillation column will maintain a temperature higher by 20 $^{\circ}$ C than the first distillation column. The pressure of the second distillation column was determined to be 2.59 bars. Some of the vapor from the top of the second distillation column is separated for use as the heat source for the reboiler from the bottom of the first distillation column so as to reduce steam and cooling water consumption by 0.6900×10^6 kcal/h. Also, by optimizing the positions of the raw material input, the heat duty for each column was minimized.

CONCLUSION

To extract normal hexane product with a purity of 95.5 wt% at a recovery ratio of 92% of the feedstock, we used a two-column configuration with a direct sequence. To conserve the hot and cold utility, i.e., respectively, steam and cooling water, a thermal integration method

was introduced. By integrating the hot vapor top stream of the second distillation column with the reboiler of the first distillation column, 0.6900×10^6 kcal/h of heat was conserved. For further energy savings, the feed tray locations of each distillation column that minimize the reboiler heat duties were determined.

ACKNOWLEDGEMENT

This study was supported by a Hongik University research fund.

SYMBOLS

- T : absolute temperature [K]
P : pressure [bar]
R : gas constant [J/gmole-K]
G : gibbs free energy [J/gmole]
x, and y_i : liquid and vapor phase mole fractions of component i and
 \hat{f}_i^v and \hat{f}_i^l : vapor and liquid phase fugacities of component i in a mixture
 γ_i : activity coefficient of component i
P_i^{vap} : pure component vapor pressure of component i
a_{ij}, b_{ij} and α_{ij} : binary interaction parameters in the NRTL model

REFERENCES

1. C. A. Floudas, *AIChE J.*, **33**, 540 (1987).
2. H. H. Cho and D. M. Kim, *Korean J. Chem. Eng.*, **24**(3), 438 (2007).
3. Simulation Science Inc., *PRO/II user guide*, South Lake Forest, USA (2001).
4. H. Renon and J. M. Prausnitz, *J. Am. Chem. Soc.*, **14**, 135 (1968).
5. G. Soave, *Chem. Eng. Sci.*, **35**, 1197 (1972).
6. D. Y. Peng and D. B. Robinson, *Ind. Eng. Chem. Fundam.*, **15**, 58 (1976).
7. G. M. Wilson, *J. Amer. Chem. Soc.*, **86**, 127 (1964).
8. D. S. Abrams and J. M. Prausnitz, *AIChE J.*, **21**, 116 (1975).
9. A. Fredenslund, A. Jones and J. M. Prausnitz, *AIChE J.*, **27**, 1086 (1975).
10. S. S. Chenm and B. J. Zwolinski, *J. Chem. Soc. Faraday Trans.*, **70**, 1133 (1974).
11. W. Beyer, H. Schubert and E. Leibnitz, *J. Prakt. Chem.*, **27**, 276 (1965).
12. H. G. Drickamer and J. R. Bradford, *Trans. Am. Inst. Chem. Eng.*, **39**, 319 (1943).